

Large-scale distribution of quasars in deep pencil-beam surveys

Andrey V. Kravtsov

Astronomy Department, New Mexico State University, Box 30001, Department 4500, Las Cruces, NM 88003-0001, USA

11 October 2018

ABSTRACT

We have used integral two-point spatial correlation function and its second derivative to analyze the distribution of quasars in three very deep surveys published in the literature. Statistically significant ($\sim 2 - 3\sigma$) correlations were found at scales of $\sim 50 - 100h^{-1}$ Mpc in all of the analyzed surveys. We have used the friend-of-friend cluster analysis to show that these correlations can be explained by the presence of relatively small quasar clusters (3 – 6 objects) which may possibly belong to larger structures such as Large Quasar Groups found in the bigger surveys. The sizes of these clusters along the redshift direction and distances between them are similar to those for structures found recently in studies of CIV absorption systems. These results present further evidence for the existence of large-scale structures at redshifts $z \sim 1 - 2$.

Key words: large-scale structure of Universe – galaxies: quasars: general.

1 INTRODUCTION

Quasi-stellar objects (QSOs) have proved to be very useful cosmological probes of the high-redshift Universe. The availability of large homogeneous surveys has made it possible to study the spatial distribution of quasars using statistical tools such as the two-point spatial correlation function. These studies have revealed that quasars are strongly clustered at scales of $r < 20h^{-1}$ Mpc^{*} (e.g. Iovino et al. 1991; Andreani & Cristiani 1992; Mo & Fang 1993; Komberg et al. 1994; Shanks & Boyle 1994 and references therein). Although there is still an ongoing discussion about whether these correlations are evolving with redshift, the fact that the amplitude and shape of the quasar correlation function are roughly similar to those of low-redshift objects (e.g. Andreani & Cristiani 1992; Mo & Fang 1993; Komberg et al. 1994; Shanks & Boyle 1994) shows that quasars may possibly be used as tracers of the matter distribution at medium redshifts ($z \sim 1 - 2$).

In addition to the statistical results, evidence has been found for structures in the quasar distribution at even larger ($\sim 100 - 150h^{-1}$ Mpc) scales (Webster 1982; Crampton, Cowley & Hartwick 1987, 1989; Clowes & Campusano 1991a, 1991b; Graham, Clowes & Campusano 1995; Komberg et al. 1996). These structures, which we call Large Quasar

Groups (LQGs), consist of $\sim 10 - 25$ quasars and have sizes and density contrasts similar to those of nearby superclusters of galaxies (Komberg et al. 1996). Recently, similar high-redshift structures have been found in the distribution of absorbers (e.g. Jakobsen et al. 1986; Sargent & Steidel 1987; Jakobsen & Perryman 1992; Dinshaw & Impey 1996; Williger et al. 1996) This indicates that supercluster type structures are observed at redshifts $\sim 0.5 - 2.5$ – the fact which may be used as a useful constraint for existing models of structure formation and evolution.

If the quasar large-scale structures are real, we should be able to detect them using statistical methods. Deng et al. (1994) used the second derivative of the integral two-point spatial correlation function to search for typical scales in the distribution of quasars. They argued that there exists a typical scale of about $95h^{-1}$ Mpc and that this scale may be related to the specific shape of the initial perturbation spectrum. In this paper we present a study of the quasar distribution in three deep surveys. We have used statistical methods similar to those of Deng et al. (1994). Our goals and strategies, however, were somewhat different. First, we have chosen to study only the deepest quasar surveys. The number density of quasars in these surveys is much higher than in the larger surveys which makes them more sensitive to the presence of structures at scales $50 - 100h^{-1}$ Mpc. Second, we have planned to look for evidence of individual large-scale structures rather than for typical scales in the overall quasar distribution (the numbers of objects in the deep samples that we used are probably too small for that).

* All the quoted scales are comoving and were calculated assuming flat Friedman cosmology with $H_0 = 100h$ km/s/Mpc and $\Lambda = 0$.

The plan of the paper is as follows: in Section 2 we present the quasar surveys and briefly discuss the limitations they impose, in Section 3 we describe the statistical methods; in Section 4 we present the results and discuss the implications in Section 5.

2 QUASAR SAMPLES

The relatively low number density of quasars in existing *bright* quasar surveys makes some of them insensitive to spatial correlations at scales $< 100h^{-1}$ Mpc (Komberg et al. 1994). On the other hand, the deepest quasar surveys usually have high enough quasar densities (mean separation between objects $\sim 20 - 40h^{-1}$ Mpc) to be sensitive to the presence of supercluster size ($\sim 100h^{-1}$ Mpc) structures. These surveys are usually composed of one or several “beams” sampling small areas on the sky. The beam sizes perpendicular to the line of sight ($\sim 30 - 50h^{-1}$ Mpc) are much smaller than the sampled distances along the line of sight ($\sim 2000h^{-1}$ Mpc). The “one-dimensional” nature of these surveys makes analysis and interpretation of the results relatively simple because if significant correlations exist, we can then look directly for the structures responsible for them. Such analysis is difficult for larger surveys because their sky geometry is usually quite complicated. However, the presently available deep surveys have small numbers of quasars (usually few tens) in a beam, which complicates and limits any statistical analysis. One then must use statistics suitable for the analysis of small data sets.

For our study we have chosen three quasar surveys published in the literature: i) a survey by Koo & Kron 1988 (hereafter KK survey), which was compiled using *UBVI* photometry, variability and proper motions of candidates; ii) a grism survey by Zitelli et al. 1992 (hereafter (ZM)²B); and iii) a deep survey by Boyle, Jones & Shanks 1991 (hereafter BJS) in which quasar selection was based on multicolor photometry of the candidates. The BJS survey is composed of three beams covering approximately the same area on the sky (≈ 0.3 sq.deg.). We have, therefore, analyzed these three beams (BJS1, BJS2, BJS3) separately. Also, following (ZM)²B, their survey can be split into two samples with different levels of completeness: a sample of 24 quasars complete to $J = 20.85$ in an area of 0.69 square degrees; and ⁽ⁱ⁾ sample of 28 quasars complete for $20.85 \leq J \leq 22.0$ in a ⁽ⁱⁱ⁾ circular area of 0.35 square degrees which is contained in the previous one. In our analysis we have used a sample of 38 quasars complete for $J \leq 22.0$ [†]. The basic characteristics of all of our samples – surveyed area in square degrees, limiting magnitude, number of quasars, and redshift interval – are presented in Table 1.

3 METHOD

In this study, we have used the integral two-point correlation function (e.g. Mo et al. 1992; Mo & Fang 1993) which is

[†] In this sample we have included all quasars inside the 20-arcmin circle defined in (ZM)²B.

Table 1. Surveys used in the analysis.

| Sample | Area (sq.deg.) | Limiting magnitude | Number of quasars | Redshift interval |
|---------------------|-------------------|-----------------------|----------------------|----------------------|
| KK | 0.29 | $B < 22.5$ | 28 | 0.9 – 3.2 |
| (ZM) ² B | 0.35 | $J < 22.0$ | 38 | 0.4 – 2.8 |
| BJS1 | 0.29 | $b_j < 21.8$ | 21 | 0.6 – 2.9 |
| BJS2 | 0.33 | $b_j < 22.0$ | 19 | 0.6 – 2.9 |
| BJS3 | 0.27 | $b_j < 21.8$ | 20 | 0.6 – 2.9 |

related to the usual differential correlation function $\xi(r)$ as follows:

$$\bar{\xi}(r) = \frac{3}{r^3} \int_0^r x^2 \xi(x) dx.$$

This choice was made because the integral correlation function is more stable than $\xi(r)$ in the analysis of small data sets. This is important because we intended to look for features in the correlation function at large scales, where signal-to-noise ratio is usually small. We estimate $\bar{\xi}(r)$ using a standard estimator (e.g. Mo & Fang 1993):

$$\bar{\xi}(r) = \frac{\Pi_{obs}(r)}{\Pi_{rnd}(r)} - 1,$$

where $\Pi(r)$ is the number of pairs with separations less than r in an analyzed sample, while $\Pi_{rnd}(r)$ is the corresponding number of pairs averaged over an ensemble of random samples. To estimate $\Pi_{rnd}(r)$, a thousand random catalogs were created using the *smoothing* method of Mo & Fang (1993). In this method, random samples are constructed by assigning each object a random position in the sky within the boundaries of the sample and by drawing redshifts randomly from a smoothed version of the original redshift distribution. The smoothed redshift distribution is obtained by averaging the number of quasars in the redshift interval $\Delta z = 0.6$ (corresponding to $\sim 500h^{-1}$ Mpc at $z \approx 1.5$) around a given redshift. This width of the interval was chosen so that it is small enough to preserve the overall survey selection envelope but is considerably larger than the scales we are interested in ($\sim 100h^{-1}$ Mpc).

The whole analysis is similar to that of Mo et al. (1992). It is outlined in the following series of steps.

First, we compute the function $\Xi(r) = \bar{\xi}(r) + 1$; Then we find the slopes $T_1(r)$ and $T_2(r)$ (or corresponding angles Θ_1 and Θ_2) of $\Xi(r)$ for every r bin using linear regression of the relation $\log \Xi(r) - \log r$ in the intervals $[r - \Delta r, r]$ and $[r, r + \Delta r]$, where Δr is the *smoothing scale*. Smoothing with a given Δr effectively damps out amplitude fluctuations in $\bar{\xi}(r)$ on scales $r < \Delta r$. The choice of Δr is determined by the mean separation \bar{r} between objects in a sample – at scales smaller than \bar{r} the shot noise is significant and must be suppressed.

⁽ⁱⁱⁱ⁾ Finally, we construct the function $\Delta\Theta(r) = \Theta_2(r) - \Theta_1(r)$, i.e. the smoothed second derivative of $\bar{\xi}(r)$. Significant changes in the slope of $\log \Xi(r) - \log r$ (changes in the shape of $\bar{\xi}(r)$) reflect the inhomogeneities in the distribution of objects at the corresponding scales. These changes result in sharp peaks in $\Delta\Theta(r)$ with scale independent amplitude (Mo et al. 1992; Deng et al. 1994). This is very useful when working on the large scales where the amplitude of the correlation function is small.

We have estimated rms errors in $\bar{\xi}(r)$ using sample-to-sample deviations in the random catalogs as well as using analytical formula presented by Mo et al. (1992). We have constructed $n = 1000$ random catalogs using the same smoothing procedure described above which we then analyzed in the same way as real data. In this way we could estimate the fluctuation in the number of pairs (and thus the fluctuation of $\bar{\xi}(r)$) at a given scale as:

$$\Delta\Pi = \sqrt{\frac{\sum_{i=1}^n (\Pi_i - \langle\Pi\rangle)^2}{n-1}},$$

here $\langle\Pi\rangle$ is the number of pairs averaged over all random catalogs, and Π_i is the corresponding number of pairs in i -th random catalog. The deviation of $\Delta\Theta(r)$ was estimated in a similar way:

$$\sigma_{\Delta\Theta} = \sqrt{\frac{\sum_{i=1}^n (\Delta\Theta_i - \langle\Delta\Theta\rangle)^2}{n-1}}.$$

These estimates were then compared with the values given by the theoretical formulae (Mo et al. 1992). For one-dimensional samples they are:

$$N_{r\pm\Delta r} = \frac{N}{2} \left(\frac{N}{L} \Delta r \right), \quad \sigma_{\Delta\Theta} = \left(\frac{2L}{\Delta r} \right)^{\frac{1}{2}} \frac{1}{N},$$

where L is the sample extent in the redshift direction, N is the number of objects in the sample, and Δr is the smoothing length adopted in the construction of $\Delta\Theta(r)$. We have found that errors predicted by these formulae agree well with values derived from the sample-to-sample variations. We have, therefore, used these formulae to estimate the significance of peaks in $\Delta\Theta(r)$.

Finally, we have used *friend-of-friend* cluster analysis (e.g. Einasto et al. 1984) to study the quasar distribution in the samples directly. The details of the cluster identification procedure and the way of estimating the probability for a cluster to be random are described in Komberg et al. (1996).

4 RESULTS

The statistics described in the previous section were computed for all five quasar samples. The functions $\Xi(r) = \bar{\xi}(r) + 1$ and $\Delta\Theta(r)$ for each sample are plotted in figs. 1 and 2. On these plots the functions are shown by solid lines and one sigma error envelope by the thin dashed lines. The features in the correlation function which we discuss below are indicated by arrows. The mean separations between quasars in the samples are $\sim 20 - 30h^{-1}$ Mpc for the KK and (ZM)²B surveys, and $\sim 40h^{-1}$ Mpc for the BJS survey. This determined the choice of smoothing length for $\Delta\Theta(r)$ – $20h^{-1}$ Mpc and $40h^{-1}$ Mpc correspondingly (on the plots $\Delta\Theta(r) = 0$ at $r < \Delta r$). The integral correlation function was computed with a bin size of $2.5h^{-1}$ Mpc for the KK and (ZM)²B samples and with a $5h^{-1}$ Mpc bin for the BJS samples. Below we describe results for each sample separately.

4.1 KK

Quasars in the KK sample show strong correlations at small scales $r < 10h^{-1}$ Mpc (fig. 1a). Statistical significance of the

correlation signal is comparable to that for samples containing ten times more quasars (e.g. Mo & Fang 1994; Boyle & Shanks 1994). While the number of objects in this sample is quite small (28), the high number density of quasars assures relatively good statistics of close pairs (see Komberg et al. 1994 for discussion of close quasar pair statistics). The same is true for the (ZM)²B sample.

The most interesting feature of the correlation function is a “bump” at $\sim 50h^{-1}$ Mpc which is also seen as a sharp negative peak in $\Delta\Theta(r)$ (fig. 1b). The significance of the peak is $\sim 2.5\sigma$. Using friend-of-friend cluster analysis we have found a quartet and two triplets (i.e. 10 quasars out of a total of 28) with sizes along the redshift direction of 43, 30, and $34h^{-1}$ Mpc correspondingly. The estimated probability for these clusters to be random is quite small for the quartet and one of the triplets (0.01 and 0.08) while for the second triplet it is rather high (~ 0.5). However, the method we use to estimate this probability is not very reliable for triplets (and does not work at all for pairs) because the uncertainty of density within the triplet is high. We have found that the excess of pairs at separations $r \sim 30 - 50h^{-1}$ Mpc (causing the bump in $\bar{\xi}(r)$) is due to the presence of these small clusters.

4.2 (ZM)²B

For this sample the correlation signal at small separations is also quite high. The “bump” is present at $\sim 110h^{-1}$ Mpc (fig. 2a) with a corresponding peak in $\Delta\Theta(r)$ (fig. 2b) which is significant at the $\sim 2.5\sigma$ level. Applying the cluster analysis, we have found three quartets and two quintets (22 quasars out of a total of 38). One of the quartets is probably random (estimated probability is ~ 0.6), the probability to be random for the rest of the clusters is small (< 0.1) – their sizes in z -direction lie in the range $25 - 50h^{-1}$ Mpc. Four of these clusters form two “pairs” $100 \pm 20h^{-1}$ Mpc creating the excess of quasar pairs at these separations.

4.3 BJS1

The statistics for the first BJS sample are shown in figs. 2a and b. There is a rise in $\Xi(r)$ at a separation of $\sim 40h^{-1}$ Mpc. This rise is not reflected in $\Delta\Theta(r)$ because its scale is equal to the smoothing scale. Using cluster analysis we have detected two clusters in this sample – a triplet and a quintet (8 out of a total of 21 quasars). The z -sizes of both clusters are $\sim 35h^{-1}$ Mpc. The estimated probability to be random is 0.05 and 0.01, respectively. Both of these clusters contribute to the excess of quasar pairs at separations of $30 - 40h^{-1}$ Mpc.

4.4 BJS2

Results for the BJS2 sample are shown in figs. 2c and d. The decay of $\Xi(r)$ at $r < 30h^{-1}$ Mpc is caused by the fact that the number density of quasars in this sample is considerably lower than in KK and (ZM)²B and even lower than in BJS1 and BJS3. This sample therefore just lacks close pairs. The correlation function fluctuates considerably at scales $\sim 150 - 200h^{-1}$ Mpc (there is a significant excess of pairs at these separations as compared to the random distribution). These

fluctuations correspond to the positive and negative peaks in $\Delta\Theta(r)$ at $\sim 150h^{-1}$ Mpc and $\sim 180h^{-1}$ Mpc. Using cluster analysis we have found a triplet (z -size $\sim 20h^{-1}$ Mpc), a quartet (z -size $\sim 20h^{-1}$ Mpc), and a sextet (z -size $\sim 75h^{-1}$ Mpc). The probability that each individual cluster is random is smaller than 0.05. Our analysis has shown that the excess of pairs at separations $150 - 200h^{-1}$ Mpc is explained by the distance between the quartet and the sextet ($\sim 180h^{-1}$ Mpc).

4.5 BJS3

The correlation function for this sample (fig. 2e) has two broad ‘‘bumps’’ at scales $\sim 100h^{-1}$ Mpc and $\sim 200h^{-1}$ Mpc. There are two negative peaks in the $\Delta\Theta(r)$ corresponding to these fluctuations (fig. 2f). Statistical significance of both peaks is $\sim 2\sigma$. The cluster analysis failed to detect any large clusters in this sample. However, the distribution of quasars in this sample is quite interesting. There are seven relatively close pairs (distances between quasars in 5 of them are less than $30h^{-1}$ Mpc and in the other two $\sim 40h^{-1}$ Mpc) separated *from each other* by either $80 - 100h^{-1}$ Mpc or $180 - 200h^{-1}$ Mpc. This causes the fluctuations in $\Xi(r)$ at the corresponding scales.

5 DISCUSSION AND CONCLUSIONS

The results presented in the previous section suggest that the distribution of quasars in the analyzed samples is not homogeneous at scales of a few tens of megaparsecs. Many quasars belong to clumps of sizes $30 - 70h^{-1}$ Mpc. The clumps are often separated by $100 - 200h^{-1}$ Mpc, which creates a pair excess at the corresponding scales. Qualitatively this quasar distribution is very similar to that of CIV absorption systems discussed in the recent paper by Williger et al. (1996). They have found that their CIV sample contains two groups of 7 and 5 absorbers of sizes $\sim 43 \times 17 \times 69h^{-3}$ Mpc³ and $\sim 25 \times 4 \times 53h^{-3}$ Mpc³ (comoving) located at $z \sim 2.3$ and $z \sim 2.5$, respectively. The distance between these two groups ($\sim 50 - 120h^{-1}$ Mpc) results in ‘‘beating’’ (the pair excess) giving rise to the correlation signal at these separations (3.5σ significance level). A number of smaller clumps were also detected. The similar clusters of CIV absorbers were also found in earlier studies by Jakobsen & Perryman (1992), Foltz et al. (1993), and Dinshaw & Impey (1996). Recently, Lespine & Petitjean (1996) presented evidences for a coherent structure extended over $\sim 80h^{-1}$ Mpc at $z \approx 2$ in the distribution of metal absorption systems. Although the numbers of CIV systems are also small, the similarity of the results may suggest that both quasars and CIV absorbers may trace the same kind of underlying structures in the matter distribution. Unlike Deng et al. (1994) we did not observe any evidence for a periodic signal in the function $\Delta\Theta(r)$ [‡]. This may be caused by the small number statistics.

The clumpy distribution of quasars in the analyzed samples is consistent with the recent studies of the quasar distribution in the larger samples (Crampton, Cowley &

Hartwick 1987, 1989; Clowes & Campusano 1991a, 1991b; Graham, Clowes & Campusano 1995; Komberg et al. 1996). These samples were found to contain several relatively rich ($\sim 10 - 25$ QSOs) groups of quasars with sizes in the redshift direction of $\sim 70 - 160h^{-1}$ Mpc. The small extent of the pencil-beam samples perpendicular to the line of sight prevents detection of such large groups. However, the detected smaller clumps can easily be parts of larger systems. It would be very interesting to check this by studying larger deep samples which are currently underway (e.g. Hall et al. 1996).

If quasars and CIV absorption systems trace the matter distribution at high redshifts as galaxies or galaxy clusters do at low redshifts, their clumpy distribution suggests that large-scale inhomogeneities similar to the nearby superclusters were already distinct at $z \sim 1 - 2$. This information may provide some useful insights into the physics of high redshift Universe. The fact that we see structures at redshifts $z \sim 1 - 2$ similar to the superclusters at $z \sim 0$ (Komberg et al. 1996), for instance, favors low-density Λ CDM or low-density CDM models in which perturbation amplitude at large scales stops growing at $z \geq 1$. On the other hand, rather high quasar-quasar correlations at small separations and high number density contrasts in the detected quasar groups may indicate that the distribution of quasars is highly biased with respect to the matter distribution. Although present available surveys are too small to provide a statistically reliable estimate of the power spectrum $P(k)$, in the future, with bigger quasar samples and better models for both QSOs and CIV absorbers, we will be able to get useful constraints on the spectrum, and thus on the theories of structure formation, for a wide range of scales and redshifts (e.g. Komberg & Lukash 1994).

6 ACKNOWLEDGMENTS

I would like to thank B.V.Komberg and V.N.Lukash for many fruitful discussions. Invaluable assistance in improving the presentation of the paper was provided by Matthew Carlson. At different stages this project was supported by an ESO C&EE grant (No. A-01-152), the Russian Foundation for Fundamental Research (project 93-02-2929), and the International Science Foundation (project code MEZ300).

REFERENCES

- Andreani, P., Cristiani, S., 1992, ApJ, 398, L13
- Boyle, B.J., Jones, L.R., Shanks, T., 1991, MNRAS, 251, 482 (BJS)
- Clowes, R.G., Campusano, L.E., 1991a, MNRAS, 249, 218
- Clowes, R.G., Campusano, L.E., 1991b, in *The Space Distribution of Quasars*, ASP Conf. Ser., **21**, D.Crampton (ed.), 248.
- Crampton, D., Cowley, A.P., Hartwick, F.D.A., 1987, ApJ, 314, 129
- Crampton, D., Cowley, A.P., Hartwick, F.D.A., 1989, ApJ, 345, 59
- Deng, Z., Xia, X., Fang, L.-Z., 1994, ApJ, 431, 506
- Dinshaw, N., Impey, C.D., 1996, ApJ, 458, 73
- Einasto, J., Klypin, A.A., Saar, E., Shandarin, S.F., 1984, MNRAS, 206, 529
- Graham, M.J., Clowes, R.G., Campusano, L.E., 1995, MNRAS, 275, 790

[‡] Although $\Delta\Theta(r)$ seems to be periodic, most of the peaks are not significant (their height is $< 1\sigma$).

Hall, P.B., Osmer, P.S., Green, R.F., Porter, A.C., and Warren, S.J., 1996, *ApJ*, 462, 614

Jakobsen, P., Perryman, M.A.C., Ulrich, M.H., Macchetto, F., Di Serego Alighieri, S., 1986, *ApJ*, 303, L27

Jakobsen, P., Perryman, M.A.C., 1992, *ApJ*, 392, 432

Iovino, A., Shaver, P., Cristiani, S., 1991, in *The Space Distribution of Quasars, ASP Conf. Ser.*, **21**, D. Crampton (ed.), 202.

Komberg, B.V., Lukash, V.N., 1994, *MNRAS*, 269, 277

Komberg, B.V., Kravtsov, A.V., Lukash, V.N., 1994, *A&A*, 286, L19

Komberg, B.V., Kravtsov, A.V., Lukash, V.N., 1996, *MNRAS*, 282, 713 (preprint astro-ph/9602090)

Koo, D.C., Kron, R.G., 1988, *ApJ*, 325, 92 (KK)

Lespine, Y., Petitjean, P., 1996, *A&A*, in press, preprint astro-ph/9606037

Mo, H.J., Deng, Z.G., Xia, X.Y., Schiller, P., Börner, 1992, *A&A*, 257, 1

Mo, H., Fang, L.-Z., 1993, *ApJ* 410, 493

Sargent, W.L.W., Steidel, C.C., 1987, *ApJ*, 322, 142

Shanks, T., Boyle, B.J., 1994, *MNRAS*, 271, 753

Webster, A., 1982, *MNRAS*, 199, 683

Williger, G.M., Hazard, C., Baldwin, J.A., and McMahon, R.G. 1996, *ApJS*, 104, 145

Zitelli, V., Mignoli, M., Zamorani, G., Marano, B., Boyle, B.J., 1992, *MNRAS*, 256, 349 ((ZM)²B)

FIGURE CAPTIONS

Figure 1. The integral two-point spatial correlation function $\bar{\xi}(r)$ for the KK (panel a) and (ZM)²B (panel c) samples and its smoothed second derivative (panels b and d) $\Delta\Theta(r)$ (see definitions in Section 3). The functions are solid lines. The 1σ error envelope is shown by thin dashed lines. The features in the correlation function discussed in the text (Section 4) are indicated by arrows.

Figure 2. The integral two-point spatial correlation function $\bar{\xi}(r)$ for the BJS1, BJS2, and BJS3 samples (panels a,c, and e, respectively) and its smoothed second derivative $\Delta\Theta(r)$ (panels b,d, and f). The structure of the plots is the same as for Fig.1.

fig. 1

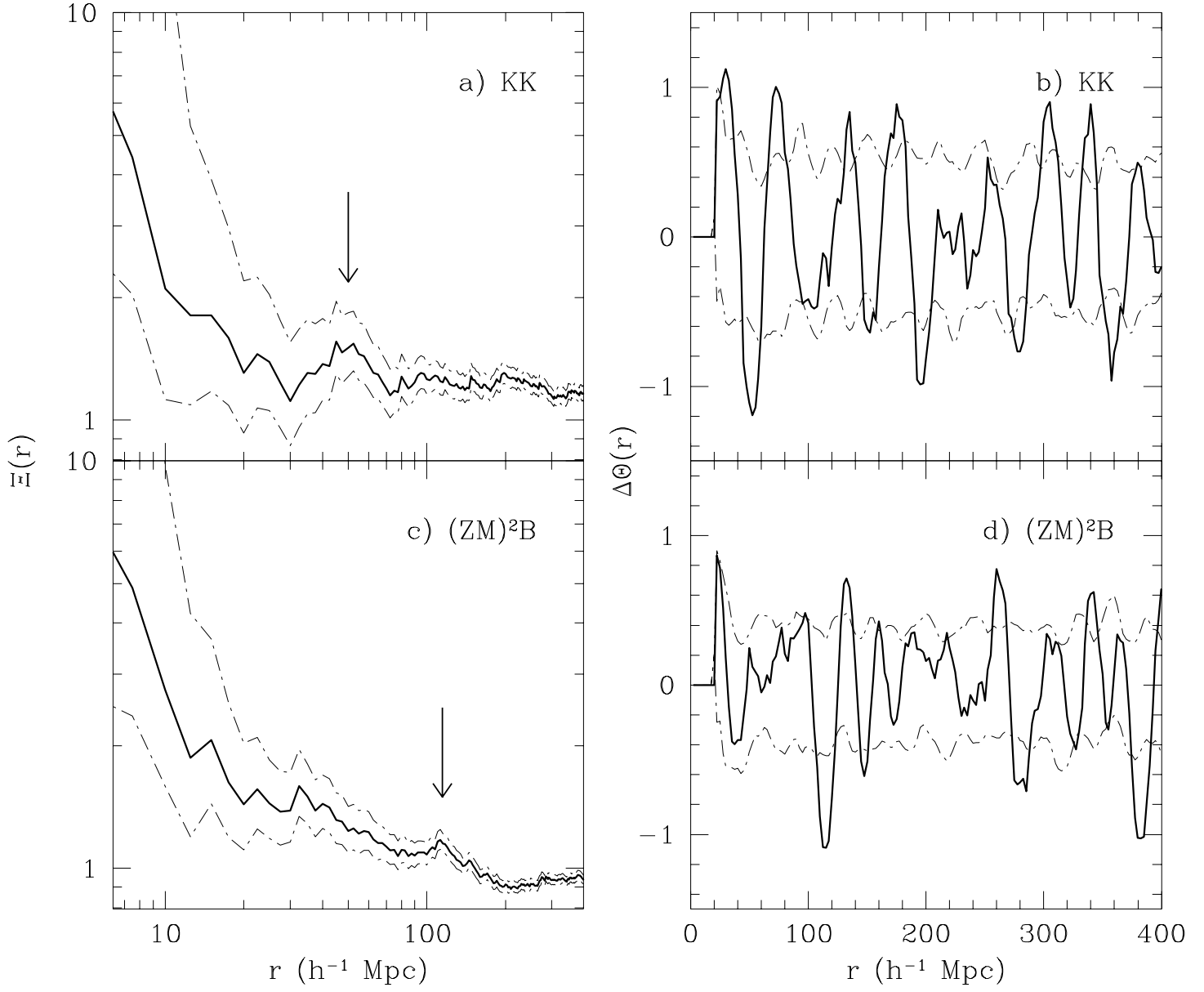


fig. 2

